frontiers | Frontiers in Earth Science

TYPE Original Research
PUBLISHED 14 February 2024
DOI 10.3389/feart.2024.1287450

OPEN ACCESS

EDITED BY
Fabio Luca Bonali,
University of Milano-Bicocca, Italy

REVIEWED BY
Hans-Balder Havenith,
University of Liège, Belgium
Nino Tsereteli,
Tbilisi State University, Georgia
Federico Pasquaré Mariotto,
University of Insubria, Italy
Francesco Muto,
University of Calabria, Italy

*CORRESPONDENCE
Yancheng Zhang,
zyc@whu.edu.cn
Jian Kuang,
kuangjian95@zedat.fu-berlin.de,
kuangjian@cug.edu.cn

RECEIVED 01 September 2023
ACCEPTED 30 January 2024
PUBLISHED 14 February 2024

CITATION
Zhou B, Zhang Y and Kuang J (2024), Historical earthquake records in the Weihe Basin, central China and new insights for geothermal genesis.
Front. Earth Sci. 12:1287450.
doi: 10.3389/feart.2024.1287450

Historical earthquake records in the Weihe Basin, central China and new insights for geothermal genesis

Bing Zhou[1], Yancheng Zhang[1]* and Jian Kuang[2,3]*

[1]College of Chinese Language and Literature, Wuhan University, Wuhan, China, [2]Department of Earth Sciences, Freie Universität Berlin, Berlin, Germany, [3]State Key Laboratory of Biogeology and Environmental Geology, China University of Geosciences, Wuhan, China

The Weihe Basin, located in central China, stands out for its significant earthquake activity while concurrently harboring promising geothermal reservoirs. The potential association between these two geological occurrences and the underlying mechanisms remain enigmatic. Here, we compile a catalog of historic earthquakes, total strain data, data related to crustal mantle structure, surface heat flow data, and heat production data of the rocks in the Weihe Basin. Our aim is to unveil the intricate interplay among the occurrence of earthquakes, tectonic activity, and the genesis of geothermal resources. Our findings reveal that earthquake activity in the Weihe Basin is regulated by the responses of faults or fractures intricately influenced by regional tectonics. These tectonic processes are responsible for the formation of favorable geothermal resources beneath the basin. We propose there is a weak zone beneath the basin, which is controlled by a combination of tectonic processes and the flow of the asthenosphere. We finally establish a comprehensive model to visualize the genesis of the occurrence of earthquakes and the formation of geothermal resources. These results have important guiding significance for future research endeavors in the realms of both geothermal exploration and earthquake investigations within the Weihe Basin.

KEYWORDS

earthquake, geothermal resources, tectonic activity, Weihe basin, geothermal genesis

1 Introduction

Geothermal energy has always played a paramount role in the sustenance and advancement of the economic development of human history. Throughout antiquity and the early stages of human civilization, human beings manifested a potential preference for settling in proximity to geothermal regions, primarily driven by the manifold applications offered by hot springs. Such geothermal resources were employed for various purposes including thermal bathing, culinary applications, the therapeutic treatment of wounds, and recreational activities (Erfurt, 2021; Wang et al., 2023). Modern societies have expanded upon the initial utilization of geothermal resources mentioned above by incorporating diverse applications such as agriculture, heating systems, power generation, *etc.* (Lund et al., 2011; Lund and Boyd, 2016; Lund and Toth, 2021). The substantial energy requirements coupled with the renewable and clean characteristics inherent to geothermal energy have led to an increased

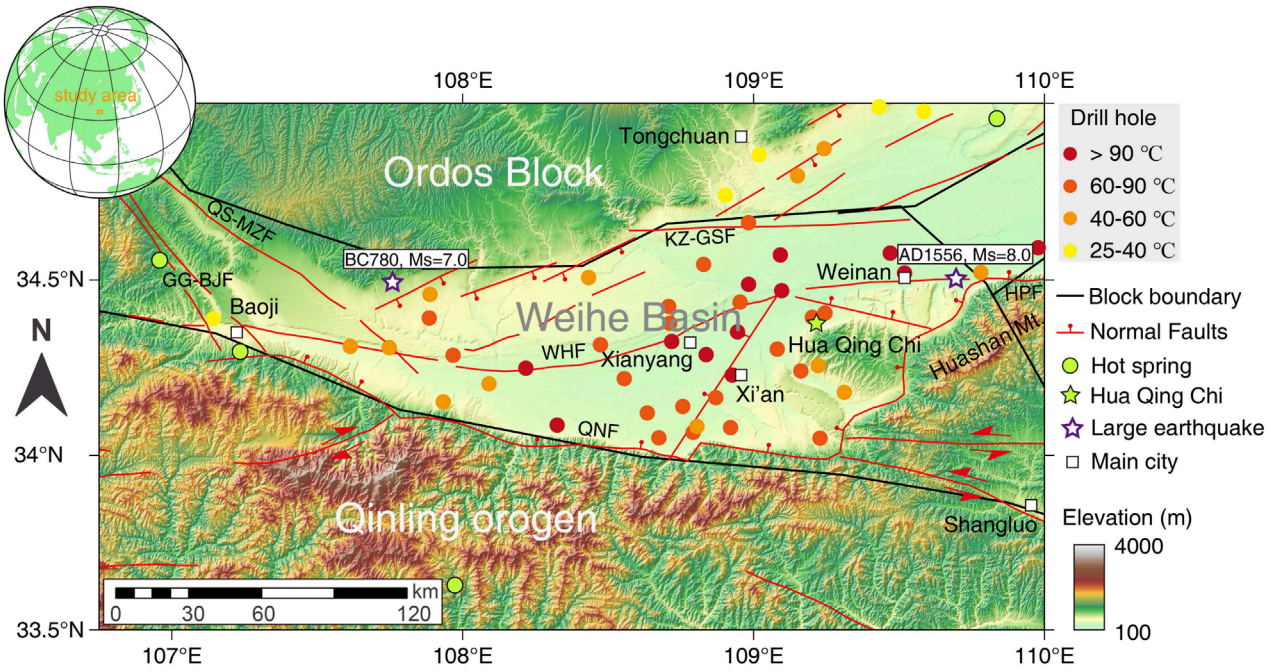

FIGURE 1
Tectonic background and topographic features of the Weihe Basin, central China. The inset shows the location of the study area. A color-shaded relief map is provided, incorporating data on active faults, earthquakes, hot springs, and geothermal drills in the Weihe Basin and adjacent areas. Locations of historic earthquakes are from National earthquake data center (https://data.earthquake.cn/). The locations and information of hot springs and geothermal drills are from Wang et al. (2020). QS-MZF, Qishan-Maozhao Fault; KZ-GSF, Kouzhen-Guanshan Fault; HPF, Huashan Piedmont Fault (one of the Qinling Piedmont fault systems); QNF, Qinling North Piedmont Fault; GG-BJF, Guguan-Baoji Fault; WHF, Weihe Fault.

growth in its utilization in recent decades (Lund and Toth, 2021; Jello and Baser, 2023).

The Weihe Basin has a significant abundance of geothermal resources and a long history of exploitation (Zhu et al., 2015). Dating back to the Western Zhou Dynasty (1100 B.C. to 771 B.C.), historical records indicate that the geothermal resources present in the region were already being harnessed by ancient residents for medicinal bathing (Xu et al., 2019). The best known is the Hua Qing Chi Hot Spring, which was built in the Tang Dynasty (618 A.D. to 907 A.D.) for the imperial thermal spa (Qin et al., 2005). Exploratory endeavors have ascertained that the sedimentary formations within the Weihe Basin have sufficient reserves of geothermal resources (Figure 1). The utilization of this resource is presently being employed on a considerable scale including heat pumps, bathing, and cultivation (Ke et al., 2021). Determining the geothermal genesis of this region is of great importance for the economic development of the area and can be applied to the discovery of its human and historical heritage.

The Weihe Basin is an earthquake active area with a rich earthquake record. There are two well-known historic earthquakes: a magnitude (*Ms*) 7.0 earthquake in 780 B.C. in the western Weihe Basin and a *Ms* about 8.0 earthquake in 1556 A.D. in Huaxian County (Figure 1). The earthquake that occurred in Huaxian in the year 1556 A.D. led to an approximate loss of 830,000 lives and extensive destruction throughout the Weihe Basin. Significant earthquake events necessitate a linkage with strong lithospheric activity (Sibson, 1986). Lithospheric activity typically couples the occurrence of hot springs/geothermal anomalies. The mantle plume activity, block friction processes, hydraulic and thermal conductivity through fractures, the upwelling of thermal material from the mantle, and the formation of highly thermally productive granites collectively represent adequate conditions conducive to the development of geothermal anomalies (Huang et al., 2015; Harðardóttir et al., 2018; Zhou et al., 2020; Ai et al., 2021). The geothermal anomalies manifested by notable geothermal resources within the Weihe Basin are intricately intertwined with lithospheric activity. However, most of geothermal genesis research in this region predominantly focuses on the observation of hot spring features in conjunction with faults. The proposed genesis of geothermal resources in the Weihe Basin is derived from a combination of hydro-chemical analyses (Luo et al., 2017; Xu et al., 2019) and published geophysical observations (e.g., Bao et al., 2011), postulating the water circulation along the faults and heat originate from mantle upwelling as contributing factors (Xu et al., 2022). There is no doubt that the occurrence of a significant number of faults and regional ruptures/fractures in the Weihe Basin (Figure 1; Cheng et al. (2018)) is intrinsically linked to regional tectonic activity (Rao et al., 2014; Lin et al., 2015). Although the earthquake catalog and records reveal the Weihe Basin as an earthquake active area (Lv et al., 2014;

Rao et al., 2014; Qu et al., 2018; Huang et al., 2022), insufficient research exists regarding the establishment of a robust correlation between tectonic activity and geothermal resources in the Weihe Basin. The potential correlation between earthquake activity and the geothermal resources in the Weibe Basin remains unestablished.

In this study, we conduct a comprehensive study of the tectonic activity observed within the Weihe Basin. Our aim is to establish a robust correlation between earthquake activity and geothermal resources by compiling historic earthquakes, total strain rate data, geophysical data linked to crustal mantle structure, surface heat flow, and heat production of rocks. We first analyze the total strain rate, supracrustal structure, and earthquake features to determine the mechanism of earthquakes in the Weihe Basin. We engage in a discussion concerning the thermal structure of the lithosphere, utilizing data derived from surface heat flow values, rock heat production rates, and crustal/lithospheric thickness. We conclude with a geothermal model to visualize the geothermal genesis in the Weihe Basin. In this model, we have established a connection between earthquakes, geothermal resources, and tectonic processes.

2 Geological setting

The Weihe Basin is located between two stable blocks/cratons and one active plateau (Figure 2A). To the north is the stable Ordos Block which has a pre-Mesozoic crystalline basement (Ma and Wu, 1987). To the south is the Qinling orogen, which were formed by the collision between the North China Craton and South China Block during the Triassic era (Wu and Zheng, 2013). To the west lies the active Tibetan Plateau, which has been moving northward to form lateral compressional stress to the eastern and southeastern Asia (Yin and Harrison, 2000). Several Cenozoic grabens/basins formed around the Ordos Block (Figure 2B) due to the Early Cenozoic extensional stress (Figure 2C) and the Late Cenozoic shear stress (Figure 2D), which were generated from the continuous northward push of the Tibetan Plateau (Shi et al., 2020). Many normal and strike-slip faults have developed in these basins due to such Cenozoic extensional and shear stress. As one of the extensional basins in a sinistral shear zone, the Weihe Basin includes the Qishan-Maozhao Fault (QS-MZF), Kouzhen-Guanshan Fault (KZ-GSF), Huashan Piedmont Fault (HPF, one of the Qinling Piedmont fault systems), Qinling North Piedmont Fault (QNF), and Guguan-Baoji Fault (GG-BJF) as its boundaries (Figure 1). The east-west striking Weihe Fault (WHF), representing the largest fault within the basin, spans across the whole basin. The Weihe Basin has undergone substantial accumulation of Cenozoic deposits reaching thicknesses of up to 7,000 m since the Eocene epoch (Liu et al., 2013). This process has been accompanied by the uplift of mountainous blocks (e.g., Huashan Mountain, Figure 1) within the region along the southern border of the Weihe Basin. The upthrown of the Huashan Mountains predominantly consist of pre-Mesozoic metamorphic basement rocks, while the Weihe Basin Loess Tableland is characterized by Quaternary loess and alluvial deposits.

3 Methods for data collection

3.1 Historical earthquakes

Due to the varying age coverage of data in different databases, the earthquake data presented in this work is derived from three distinct databases. Earthquake data spanning from 1970 to the present can be acquired from online databases. The earthquake records from present to the 2009 are from the National earthquake data center (https://data.earthquake.cn/). The earthquake records between 1970 and 2009 are from the USGS (https://earthquake.usgs.gov/earthquakes/search/). Earthquake data predating 1970 is not accessible through online databases but is exclusively retrievable from recorded content in (ancient) books. Books typically document large and perceptible earthquakes, leading to an incomplete data coverage in many cases. We first conducted a statistical analysis of historic earthquakes in the Weihe Basin and its surrounding areas mainly using three books: the atlas of the historical earthquakes in China (from ancient period to Ming Dynasty), the atlas of the historical earthquakes in China (Ming Dynasty), and the atlas of the historical earthquakes in China (Qing Dynasty) (Institute of Geophysics, 1986). These three books primarily present ancient textual accounts of earthquakes, extrapolated magnitudes derived from documented post-earthquake phenomena, and possible latitude and longitude of the epicenter. We then explored the Chinese Basic Ancient Books Library (http://old.lib.whu.edu.cn/download/ClientSetup.rar), Dingxiu Ancient Books Full Text Retrieval Platform (http://www.ding-xiu.com/ancientbook/portal/index/index.do), and the Shutongwen Ancient Books Database (https://guji.unihan.com.cn/) using location-based keywords "Xi'an", "Xianyang", and "Guanzhong Basin", and ancient Chinese terms synonymous with earthquake to supplement and rectify the previously acquired data. Incomplete latitude and longitude values were supplemented using Google Earth. Finally, we filtered the acquired data to retain information that aligns with the scope of the study area outlined in this work.

The focal mechanism data of earthquakes in the Weihe Basin from 2009 to 2021 is from Guo et al. (2022) and is presented in this study as well.

3.2 Lithospheric structure

The lithospheric structure data encompasses information on total strain rates, sediment thickness, crustal thickness, and lithospheric thickness.

The only available data of the total strain rate involved in the study area comes from Kreemer et al. (2014). We discretize the data and utilize it as the total strain rate field for the study area.

The sediment thickness data is derived from drill hole data. The contour data for sediment thickness was presented in Yi (1993), relying on data from 30 drill holes.

The data on crustal and lithospheric thickness data are obtained from local geophysical inversion data in China. We choose data from the latest research results to effectively constrain the lithospheric structure of the Weihe Basin and its surrounding areas. For the

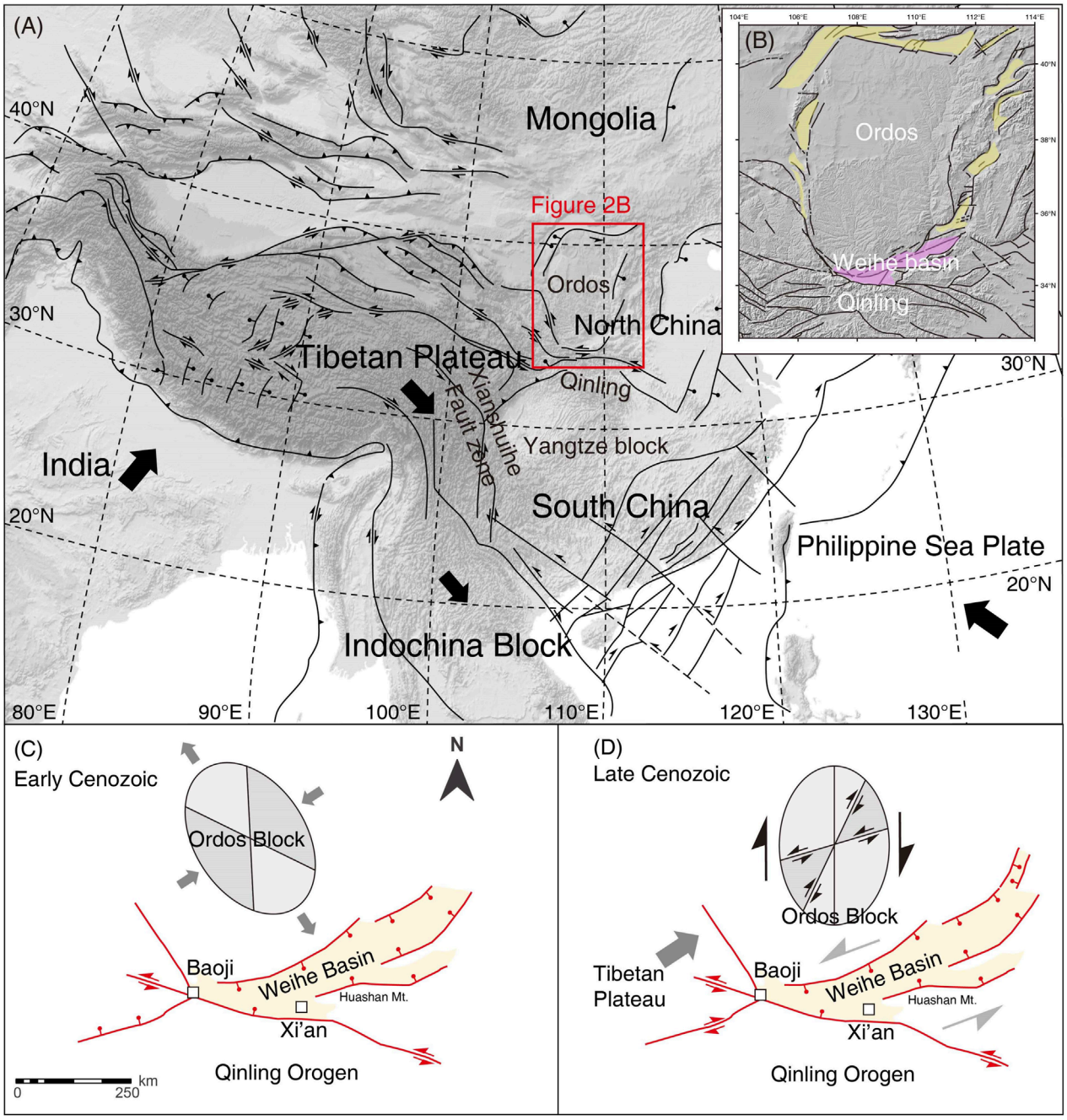

FIGURE 2
Tectonic evolution of the Weihe Basin. **(A)** Tectonic map of Asia (modified from Kuang et al. (2020)). The black lines are the faults and blocks boundaries. The outlined red rectangle is the location of Figure 2. **(B)** Tectonic map of Ordos Block and surrounding areas. The purple shaded area is the Weihe Basin. The yellow shaded areas are the rifted basins around the Ordos Block (Modified from Su et al. (2023)). **(C)** Early Cenozoic evolution of the Weihe Basin and Ordos Block (modified from Shi et al. (2020)). The ellipsoid represents the force state of the Ordos Block. Extensional force forms normal faults in the Weihe Basin. **(D)** Late Cenozoic evolution of the Weihe Basin and Ordos Block (modified from Shi et al. (2020)). The ellipsoid represents the force state of the Ordos Block. Shear force forms strike-slip faults in the Weihe Basin.

crustal thickness of the Weihe Basin and adjacent areas, the data are from Feng et al. (2017). For the lithospheric thickness of the Weihe Basin and adjacent areas, the data are from Deng and Levandowski (2018).

3.3 Lithospheric thermal structure

The thermal structure of the lithosphere is usually obtained using the 1-D steady-state equation (Hasterok and Chapman, 2011).

In a steady thermal state of lithosphere, temperature (T), heat flow (q), heat production rate (A), thickness of selected layer (Δd), thermal conductivity (λ) can be written as Eq. 1,

$$T_{i+1} = T_i + \frac{q_i}{\lambda_i}\Delta d_i - \frac{A_i}{2\lambda_i}\Delta d_i^2$$

and equation (2)

$$q_{i+1} = q_i - A_i \Delta d_i$$

The heat production rate (A) is determined by rock concentration of Th, U, K_2O,

$$A = 10^{-5}\rho\left(3.5C_{K_2O} + 9.67C_U + 2.63C_{Th}\right)$$

with concentrations of K_2O in wt%, and of U and Th in ppm. We adapt a density, ρ, value of 2,677 kg·m^{-3} of rocks in the upper crust. We calculate the heat production rate (A) by employing rock data from the compiled igneous rock database by Hasterok and Webb (2017) and the GEOROC database (https://georoc.eu/georoc/new-start.asp).

The surface heat flow data (q) in the Weihe Basin and adjacent areas are from the International Heat Commission database (http://www.ihfc-iugg.org/products/global-heat-flow-database). We discretize the heat flow map, which serves as the data source for the analysis in the work.

4 Results

4.1 Historical earthquakes

A total of 212 earthquakes have been compiled in this work. All data are presented in Supplementary Table S1 and shown in Figure 3. Historical records indicate a total of 32 earthquakes with $Ms \geq 4$ from 780 B.C. to present in the Weihe Basin (Figure 3A). The most significant earthquake, reaching a magnitude of 8, took place in Huaxian in the year 1,566. After the year 1800, the region has not experienced any earthquakes with a magnitude exceeding 6. Over the past decade, more than 180 earthquakes with $Ms \geq 1$ and several felt earthquakes have been recorded in this region. The focal depth of these earthquakes is less than 30 km, with a significant majority falling within the range of 5–10 km (Figure 3B). Notably, there are almost no earthquakes occurring at shallow depths within 4 km (only 1 data). As shown by Figure 3C, large earthquakes ($Ms > 4$) are generally occurring along the faults, especially along the Weihe Fault. The distribution of small earthquakes ($Ms < 4$) in the region is not markedly associated with faults or block boundaries. From the perspective of earthquake occurrence mechanism, as displayed by the seismic beach ball in Figure 3C, earthquakes that occur along the northern and southern borders of the basin are mainly generated by strike-slip faults, while earthquakes occurring within the interior of the basin are generated by normal faults. Summarizing the above, the abundance of earthquakes in the Weihe Basin implies the presence of distinctive and strong tectonic activity in the region.

4.2 Lithospheric structure

As shown in the total strain rate map of the Tibet Plateau and its surrounding areas (Figure 4A), the Weihe Basin is situated at an intersection of both high and low strain rates (Figure 4A). To the west of the Weihe Basin is the Tibet Plateau, which is generally located at a high total strain rate. To the north of the Weihe Basin is the Ordos block with extremely low internal total strain rate, to the east is the North China Craton with low internal total strain rate, and to the south is the South China block with almost zero internal total strain rate. The Weihe Basin is located at the periphery of these geological blocks and has a comparatively high total strain rate. There are two extreme total strain rate areas in the eastern and western parts of the basin (Figure 4B). These extreme values are considerably lower than the total strain rate values at the boundary between the Weihe Basin and the Ordos Block to the north. However, they are higher than the total strain rate values at the boundary between the Weihe Basin and the South China Block to the south. The overall trend of the basin is from north to south, with a decrease in the total strain rate value.

The Weihe Basin is characterized as an asymmetric Cenozoic graben. This basin comprises two depocenters, one located to the north of Weinan City and the other to the west of Xianyang City. It exhibits deeper features in the south and shallower features in the north (Figure 4C). The sedimentary cover in the southern part of the basin has a thickness of more than 6,000 m, whereas the northern part of the basin has a thickness of approximately 4,000 m. The southern region of the basement surface showcases steeper characteristics, while the northern area displays a gentler inclination (Figure 4D). The overlying sediment cover is composed of Quaternary mud and sandy clay, Neogene mudstone, and Paleogene mudstone. Lithologic units below the cover are composted by pre-Cenozoic granites, gneiss, and limestone (Ren et al., 2020).

On the lithospheric scale, the Weihe Basin has a relatively thin crust, measuring approximately 40 km in thickness compared to its surrounding areas (Figure 4E). This value is consistent with other data obtained by receiver function, shear-wave, seismic reflection, and other geophysical methods (Tang et al., 2015; Si et al., 2016; Feng et al., 2017; Deng and Levandowski, 2018; Ai et al., 2019; Liang et al., 2022). However, the thickness of the lithosphere of the Weihe Basin shows no significant deviation from the surrounding lithospheric thickness. Furthermore, the overall thickness of the lithosphere of the Weihe Basin is relatively substantial, measuring around 140 km (Figure 4F). This value is comparable with other results from many recent geophysical studies (An and Shi, 2006; Li et al., 2013; Zhang et al., 2022). Therefore, the data regarding the thickness of the crust and lithosphere used in our analysis is considered reliable.

4.3 Heat flow and heat production rate

The Weihe Basin has a relatively high surface heat flow with an average value of ~70 mW·m^{-2} (Figure 5A). This is consistent with the observed surface heat flows ranging from 55 to 93 mW·m^{-2}, with an average value of 68 mW·m^{-2} (Ren et al., 2020). Such values are lower than the average surface heat flow of the Cenozoic basin in eastern China (>70 mW·m^{-2}, Jiang et al. (2019)), and higher than that of Chinese continental (61.5 mW·m^{-2}, Jiang et al. (2019)) and global continental (67 mW·m^{-2}, Lucazeau (2019)). A positive correlation exists between the surface heat flow in the interior of the basin

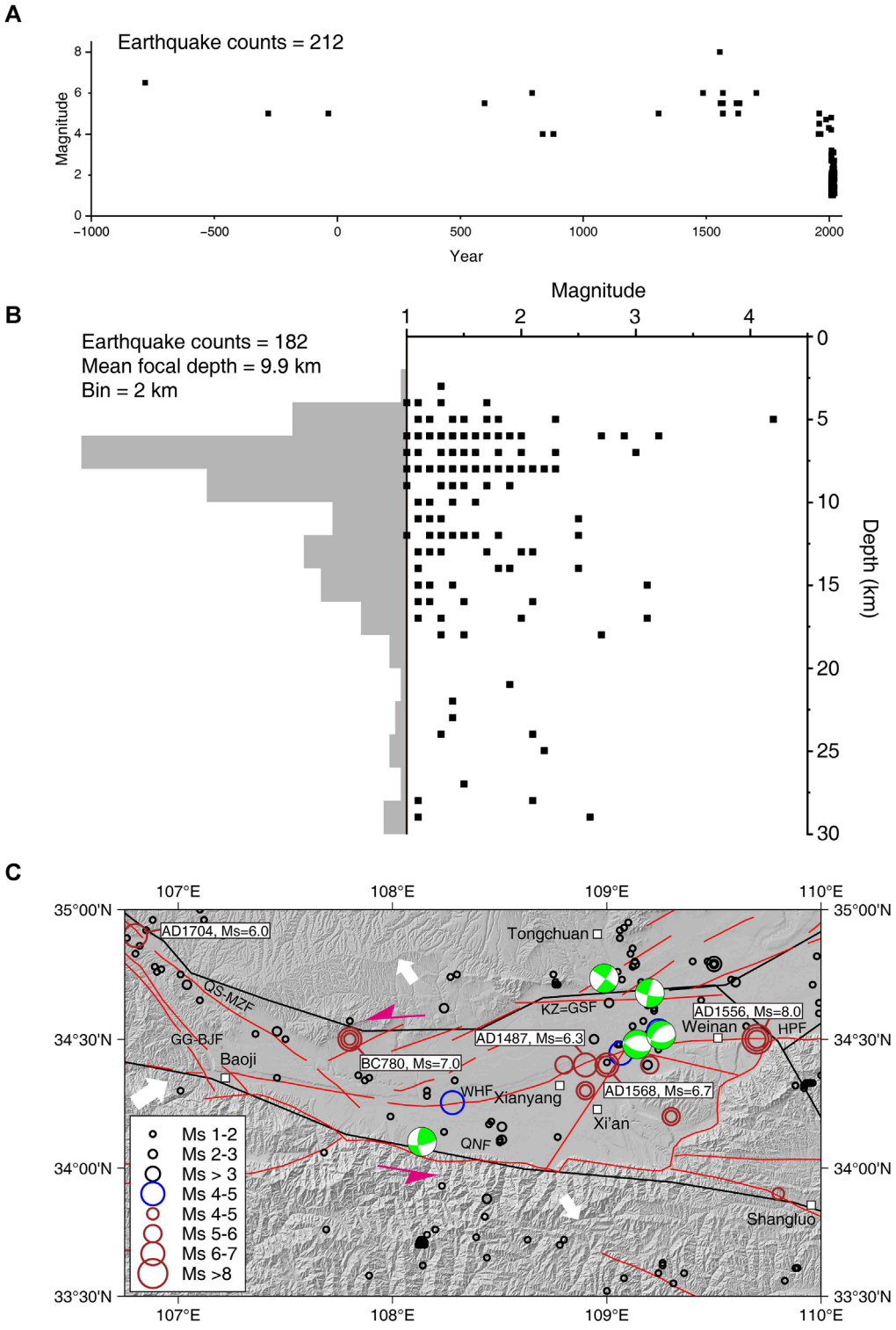

FIGURE 3
(A) Relationship diagram between historical earthquakes, magnitude, and year. **(B)** The profile of earthquakes records from 2009 to present. Earthquake data from National earthquake data center (https://data.earthquake.cn/). **(C)** The distribution of historical earthquakes. The red circles, blue circles, and black circles are the earthquake records before 1970 year, from 1970 year to 2009, and from 2009 to present. The beach balls represent the focal mechanism of some earthquakes (data from Guo X. et al. (2022)). The white and pink arrows represent the stress field of the Weihe Basin. The black lines are the boundaries of blocks. The abbreviation of faults is consistent with Figure 1.

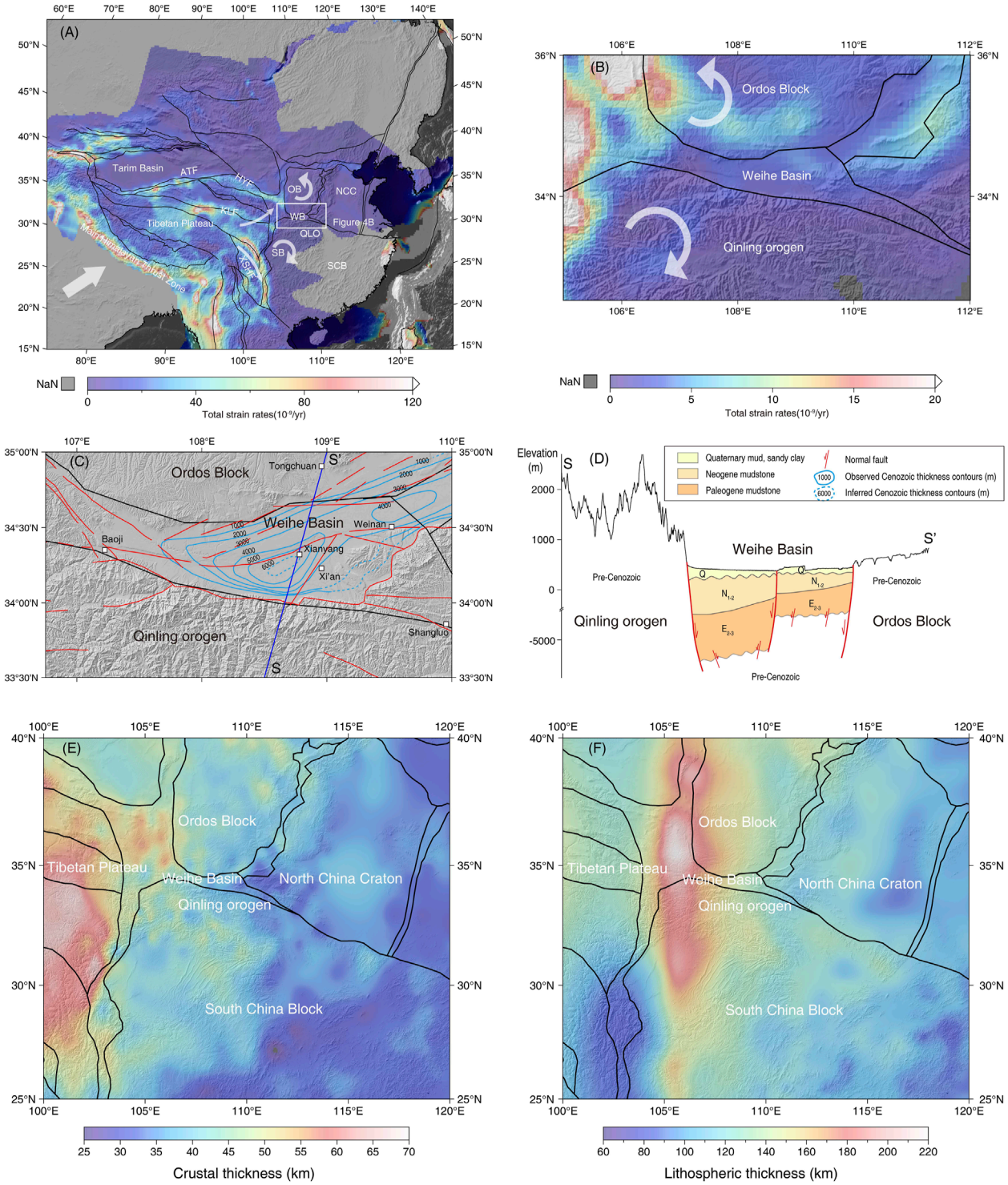

FIGURE 4
(A) Strain rates field in the Tibetan Plateau and adjacent areas. Total strain rates data from the Global Strain Rate Model (Kreemer et al., 2014). The black lines are the boundaries of blocks. The white arrow represents the rotation direction of blocks (Arrows in Xianshuihe Fault zone and Sichuan Basin are modified from Todrani et al. (2022); Tong et al. (2018); Arrow in Ordos Block is modified from Su et al. (2021); Zhang et al. (2018)). ATF, Altyn Tagh Fault; HYF, Haiyuan Fault; KLF, Kunlun Fault; XSHF, Xianshuihe Fault zone; OB, Ordos Block; WB, Weihe Basin; QLO, Qinling Orogen; SB, Sichuan Basin; SCB, South China Block; NCC, North China Craton. **(B)** The strain rate field in the Weihe Basin and adjacent areas. The black lines are the boundaries of blocks. The white arrow represents the rotation direction of blocks. **(C)** Thickness contours of Cenozoic strata in the Weihe Basin. The contours data from Yi (1993). The dark blue solid line shows the section location in the Weihe Basin. The black lines are the boundaries of blocks. **(D)** Section in the Weihe Basin. Section S-S′ is marked in Figure 4. **(E)** Lithospheric thickness of the Weihe Basin and adjacent areas. Data from Deng and Levandowski (2018). The black lines are the boundaries of blocks. **(F)** Crustal thickness of the Weihe Basin and adjacent areas. Data from Feng et al. (2017). The black lines are the boundaries of blocks.

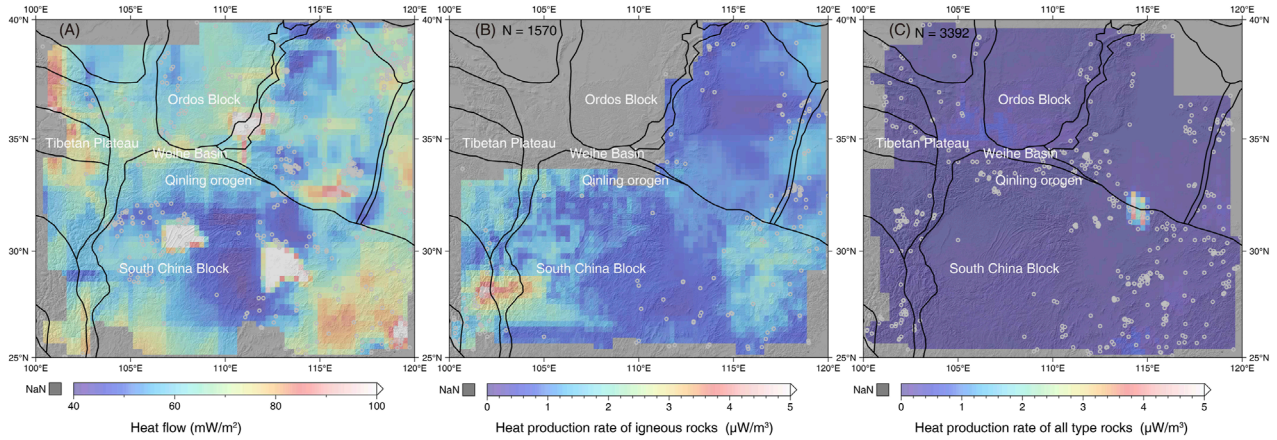

FIGURE 5
(A) The interpolated values for the surface heat flow in the Weihe Basin and adjacent areas. Values are from the International Heat Commission database (http://www.ihfc-iugg.org/products/global-heat-flow-database). The black lines are the boundaries of blocks. The interpolated values for the radiogenic heat production of surface igneous rocks **(B)** and all types of rocks **(C)**. Igneous rock data from the compiled igneous rock database by Hasterok and Webb (2017). The data of all types of rocks in this area from the GEOROC database (https://georoc.eu/georoc/new-start.asp). The black lines are the boundaries of blocks.

and the thickness of the Cenozoic cover, with the maximum heat flow occurring in the deepest part of the basin. The Weihe Basin is also in a conjunction between low surface heat flow areas of South China Block, Ordos Block, and west of North China Craton (Figure 5A). These characteristics make the Weihe Basin inherently a thermal basin.

As displayed in Figures 5B, C, the rocks near the Weihe Basin, whether igneous or all type rocks, have low rates of heat production (~1 μW/m^3). Such values are comparable to the average heat production rate of the upper continental crust (1.67 μW/m^3, data calculated from Rudnick and Gao (2003)) and considerably lower than the typical heat production rate of granite (>3.1 μW/m^3 (Paternoster et al., 2017)), which is known for its efficacy as a heat source.

5 Discussions

5.1 Potential mechanism of the earthquakes

The interaction among multiple blocks results in the Weihe Basin being located within a region of relatively high strain rate. The ongoing India-Eurasia collision, coupled with the continuous northward push of the Indian Plate, has created the Tibetan Plateau, which represents the largest deforming area on Earth and is characterized by widespread tectonic activity (Molnar and Tapponnier, 1975). GPS observations indicate that blocks within East Asia are moving in the east and southeast directions (Wang and Shen, 2020). Geophysical observations suggest an eastward mantle flow (Hirn et al., 1995; Huang et al., 2015) coupled with crustal flow (Clark and Royden, 2000). Distinct strain rates regionally characterize block motions of diverse nature (Fagereng and Biggs, 2019). The highest total strain rates are calculated along the Main Himalayan Trust zone (the core of the Indian-Eurasian collision zone), followed by the Pamir tectonic syntax at the western boundary of the Tibetan Plateau, the Altyn Tagh Fault and the Haiyuan Fault to the northern boundaries, and the Xianshuihe Fault Zone to the eastern boundary (Figure 4A). Inside the Tibetan Plateau high strain rate areas are concentrated along the Kunlun Fault zone, which is the boundary between the Qidam Block and the Qiangtang Block. The boundaries of geological tectonic units are the areas of most intensive deformation coupled with the occurrence of earthquakes. For example, an arc-like clockwise rotation pattern was formed from the Xianshuihe Fault zone to the Indochina region through the Ailaoshan-Red River fault zone (Figure 4A; Todrani et al. (2022)). As the outermost end of the arc-like clockwise rotation, the Xianshuihe Fault zone bears the most significant total strain rates. The Xianshuihe Fault zone is a favorable area for the occurrence of large earthquakes (Li and Bürgmann, 2021). This boundary influence effect is widespread within the boundary zone of the Tibetan Plateau (Wang and Shen, 2020). Although the Ordos Block is located near the boundary zone of the Tibetan Plateau, it exhibits an almost negligible total strain rate within its interior due to the sheltering by its stable craton property. However, since the Ordos Block is influenced by the northern motion of the Tibetan Plateau, the peripheries of the Ordos Block have a high total strain rate (Figure 4A). There are also numerous historically large earthquake records in the peripheries of the Ordos Block (Wang and Shen, 2020). The Weihe Basin is positioned between two stable Blocks (Ordos Block and South China Block) and one active tectonic unit (Tibetan Plateau). The collision of the India-Eurasia plates, leading to the eastward direction motion of blocks and anti-clockwise rotation of the Ordos Block and clockwise rotation of the South China Block (Figure 4A), subjected the junction of blocks (Weihe Basin) to relatively high total strain rates (Figure 4B). This junction of force contributes to the formation of the Weihe Basin (Figures 2C, D). The formation of the Weihe Basin was accompanied by the development of many faults (Shi et al., 2020). Fault systems evolve with increasing total tectonic displacement, with tectonic

shear deformation progressively localized at major faults (Kato and Ben-Zion, 2021). Within fault zones in the Weihe Basin, internal blocks undergo deformation processes, including stepovers and bends, when subjected to relatively high total strain rate (Figure 4B), culminating in the occurrence of earthquake events.

Fault features govern the occurrence of different types of earthquakes. Under the influence of multiple blocks, the Weihe Basin inherently adopts the characteristics of a pull-apart basin. Consequently, faults at the basin's periphery should primarily undergo shear stress, while the interior of the basin will be predominantly subjected to extensional stress. This statement is confirmed by the seismic beach ball in Figure 3C. Earthquakes occurring at the basin's periphery are primarily attributed to the activity of strike-slip faults, while earthquakes within the basin are induced by the activity of normal faults.

The mechanism of earthquake occurrence can also be discerned from the distribution of focal depth and supracrustal structure. The shallow crust in the Weihe Basin is extensively fractured and cut by normal faults (Figure 1). As discussed in Section 2, the Weihe Basin was formed by extensional stress from the motion and rotation of the South China Block and Ordos Block. The entire basin is dissected into several smaller geological units due to the presence of interconnected normal faults. These normal faults exhibit varied offsets within the basin. As shown by the focal depth of earthquakes (Figure 3B), almost all earthquakes in this region have a focal depth greater than 5 km, while the depth of the sedimentary basin is less than 5 km in most areas. This robust correlation suggests that earthquakes are likely to occur during tectonic activity within the basement. We suggest that, despite being intersected by many faults, the sedimentary basin is generally stable. Conversely, the geological units beneath the sedimentary basin are a favorable zone where earthquakes occur more frequently. The diminishing occurrence and intensity/magnitude of shallow to deep earthquakes suggest a gradual enhancement in the stability of the block with depth. Inferred from the distribution of focal depth, the active depths of faults are primarily concentrated at upper-mid-crustal levels, particularly within the upper crust. Combined with the results mentioned above, it is clear that the shallow crust of the Weihe Basin has undergone extensive fracturing or faulting due to regional stresses and tectonics, whereas only a minute proportion of these faults extend into the lower crust and even reach down to the mantle (for example, the Weihe Fault, Tang et al. (2015)).

In summary, the stress resulting from regional block activity in the Weihe Basin accumulates within the basin, subsequently triggering widespread fault activity and resulting in the occurrence of earthquakes.

5.2 Regional lithospheric thermal structures near the Weihe Basin

Surface heat flow is a critical parameter for interpreting the lithospheric thermal structure (Furlong and Chapman, 2013). We begin our analysis with the premise that heat from the deeper part of the Weihe Basin reaches the surface only through thermal conduction. We use the steady state geotherm families of lithosphere computed by Pollack and Chapman (1977) and Hasterok and Chapman (2011) to analyze the lithospheric thermal state in the Weihe Basin. Since the key parameters of published surface heat flow and thermal conductivity and density of different types of rock in the Weihe basin (Ren et al., 2020) and the Moho depth (~40 km, Figure 4E) are almost the same of that used by Pollack and Chapman (1977) and Hasterok and Chapman (2011), we reasonably postulate that the lithospheric geotherms are equally applicable in analyzing the thermal state of the lithosphere within the Weihe Basin. The surface heat flow values in the Weihe Basin correspond to a thermal lithospheric thickness ranging from 44 to 102 km with an average of 73 km, derived from a standard lithospheric geotherm with a heat production partition factor of 0.26 (Figure 6A). This inferred thermal lithospheric thickness values are lower than the lithospheric thickness (~140 km, Figure 4F) and the proposed thermal lithospheric thickness (90–100 km (Liu et al., 2016; Xu et al., 2020)). Based on equation (1) and (2), for a constant temperature, heat production rate, and thermal conductivity, the surface heat flow decreases with an increase in the thickness of the lithosphere, as observed on our planet (Furlong and Chapman, 2013). Therefore, higher heat flow coupled with to thicker lithosphere requires high crustal heat production rate at a steady thermal state (Figures 6A, B). Furthermore, the heat production partition factor should be at least greater than 0.4 (Figure 6B), based on the ~140 km lithospheric thickness (Figure 4F). However, the rock heat production rate in the Weihe Basin and its surrounding areas is low (Figures 5B, C), even falling below the global average level for the upper crust. Given our assumption that heat reaches the surface only through thermal conduction, the low heat production rates are insufficient to account for the thermal basin phenomenon observed beneath the thick lithosphere in the Weihe Basin.

Another solution is thermal convection as another principal mechanism of subsurface heat transfer within the Weihe Basin. As mentioned in Section 4, the abundance of normal faults in the subsurface of the Weihe Basin could serve as favorable pathways for fluid migration. The fracture zones containing fluids may also manifest as low resistivity bodies detected in geophysical observations (Zhao et al., 2021; Li et al., 2022; Liang et al., 2022; Yang et al., 2022). The correspondence between the thermal structure and lithospheric structure further substantiates the validity and reasonability of our analysis in this context.

Summarizing the above, the lithospheric thermal structure is not homogeneous, as heat is transferred to the surface through a combination of conduction and convection beneath the Weihe Basin. This mode of heat transfer is intimately linked to the lithospheric structure and is predominantly influenced by the presence of extensive normal faults or fractures resulting from regional tectonics. The fluids accomplish heat transformation (thermal convection) in the fracture voids.

5.3 Geothermal genesis model in the Weihe Basin

Considering the preceding synthesis and discussion, a conceptual model is proposed to describe the formation and evolution of geothermal resources in the Weihe basin (Figure 7). This model comprehensively outlines the geothermal genesis of the Weihe Basin, taking into consideration both the lithospheric structure and thermal structure.

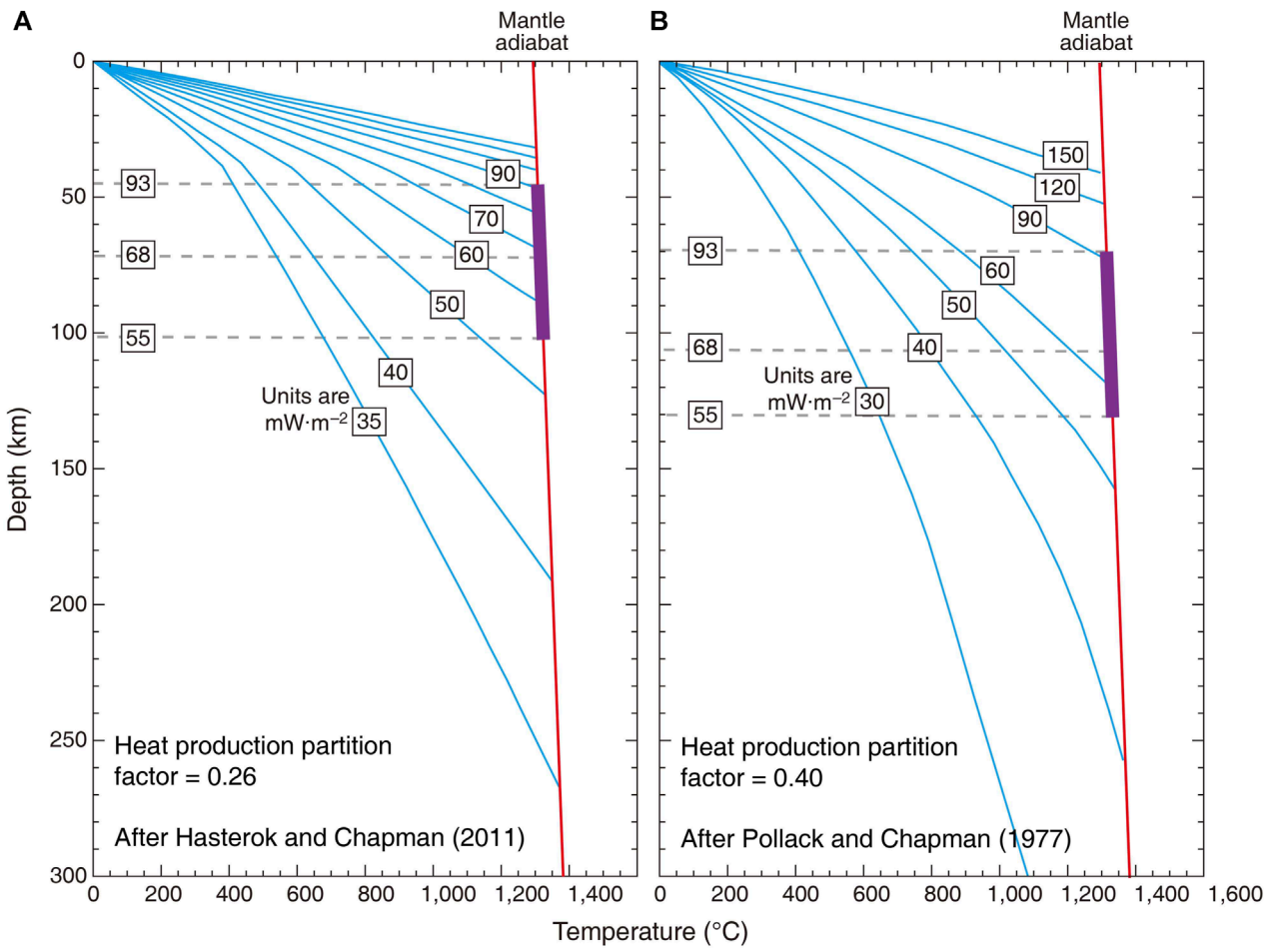

FIGURE 6
(A) Lithosphere-scale geotherms for continental regions. Geotherms developed by Pollack and Chapman (1977) employing a heat production partition factor of 0.4 and an exponential decrease of heat production in the upper crust. **(B)** Lithosphere-scale geotherms for continental regions. Geotherms presented by Hasterok and Chapman (2011) applying a heat production partition factor of 0.26 and constant heat production in the upper crust. Purple solid line shows the maximum, minimum, and average value of surface heat flow in the Weihe Basin.

The origin of geothermal heat sources in the Weihe Basin is diverse and can be categorized into two main components: heat from the crust and heat from the mantle. Crustal heat sources predominantly stem from the radiogenic decay of heat-producing elements in granite (Bea, 2012), the release of heat from magma chamber (Gillis, 2008), and the generation of frictional heat within fracture zones (Ai et al., 2021). According to the insights provided in Section 5, the radiogenic decay of heat-producing elements in igneous rocks and other rocks is not sufficient as a source of heat for geothermal genesis. Historical records of volcanic eruption in ancient and modern China (Chen and Chen, 2021) and active volcano lists in China (Xu et al., 2021) collectively disregard the existence of active volcanoes near the Weihe Basin. Indeed, geophysical observations have identified some low-velocity geological units beneath the Weihe Basin (Zhao et al., 2021; Li et al., 2022; Liang et al., 2022; Yang et al., 2022) that might potentially indicate magmatic activity (e.g., the occurrence of magma chamber). However, the absence of magma signature, for example, without a high $^{3}He/^{4}He$ value (Zhang et al., 2019; Chen et al., 2023), does not support the existence of magma chamber. Thus, we believe that these observations are more plausibly linked to fault zones influenced by the presence of fluids, given the low-velocity characteristics exhibited by the fault zones. The plausible heat sources include frictional heat within fracture zones and heat from the mantle. Geodetic data, including GPS and satellite data, reveal that the blocks surrounding the Weihe Basin have a velocity of about 10 mm/yr, characterized by ongoing eastward horizontal motion (Hao et al., 2016; Wang and Shen, 2020; Tian et al., 2023). The vertical velocity field, derived from the remote sensing data, indicates the maximum subsidence and uplift both occurred over the Weihe Basin at rates of approximately −146 and 20 mm/yr, respectively (Qu et al., 2022). The combination of lateral and vertical block movements results in medium-high slip rates (2.1–5.7 mm/yr) of faults within the Weihe Basin (Rao et al., 2014; Huang et al., 2022). The Weihe Basin and its surroundings predominantly lie on an unstable block, with a notable history of large earthquakes reported within or around the study area over the historical period (Figure 3). All the recorded data points to the activity of faults in the Weihe Basin, leading to the

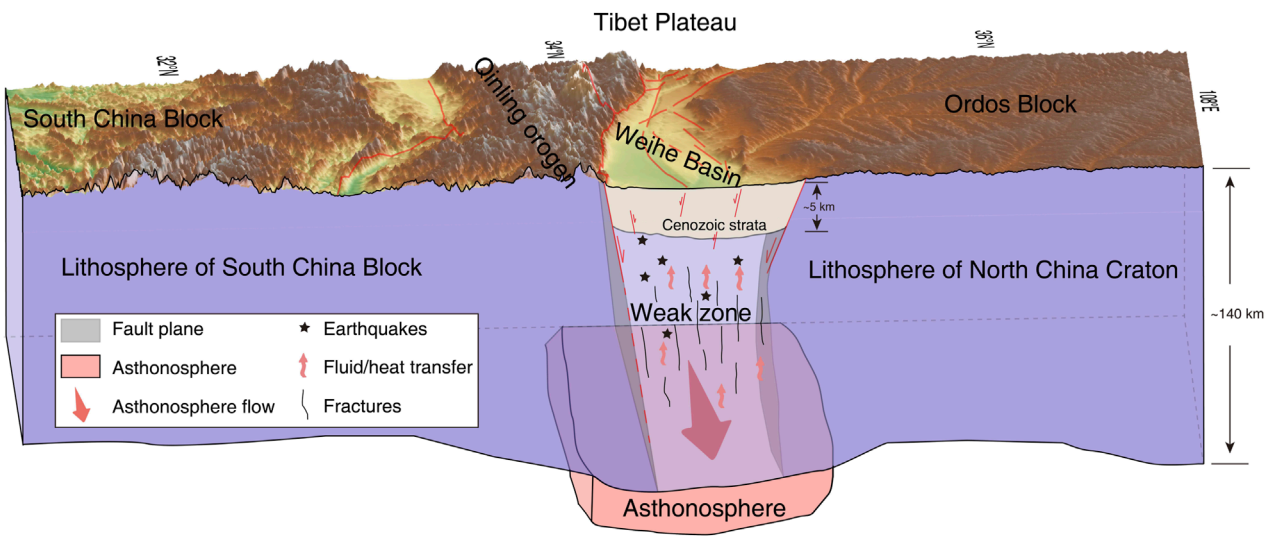

FIGURE 7
The concept geothermal genesis model in the Weihe Basin. The red lines are the faults.

generation of frictional heat due to the movement of faults. The heat from the mantle primarily propagates to the surface through thermal conduction, as there is no evidence of mantle material upwelling. Based on the analysis of heat flow data in China (Jiang et al., 2019) and the discussion presented in Section 5, it is inferred that the proportion of mantle heat in the heat source of the Weihe Basin is lower than that of crustal heat.

The existence of weak zones facilitates the generation and transfer of heat. The Weihe Basin, along with the Qinling orogen, is situated in the convergence zone between the North China Craton and the South China Block, where the yield strength is lower than that of the two stable blocks (Zhang et al., 2022). The collision between the Indian and Eurasian plate, leading to the rotation of these two blocks (Figure 4A), has resulted in a significant number of faults and fractured zones at the junction (Weihe Basin). The northward subduction of the Indian Plate, combined with the resistance from the Tarim lithosphere (Tang et al., 2023), triggers eastward movement of the asthenosphere (Yin and Taylor, 2011). Such eastward asthenosphere flow has been observed in the east part of the Tibet Plateau by various geophysical methods (Huang et al., 2015; Yu and Chen, 2016; Huang and Chevrot, 2021). The eastward flow of the asthenosphere has also been detected beneath the Weihe Basin, adjacent to the eastern Tibetan Plateau (Huang et al., 2008; Guo and Chen, 2016; Yu and Chen, 2016; Yu et al., 2021; Guo et al., 2022; Wu et al., 2022). The ongoing process of mantle flow induces thermal-chemical erosion of the lithosphere beneath the Weihe Basin. The erosion process leads to the reworking of the overlying lithosphere, which was originally weakened by tectonics and characterized by fractures. The presence of higher total strain rates (Figures 4A, B) and active structures (Figures 1, 3C) in this weak zone increases the probability of earthquakes occurring. The occurrence of earthquakes is induced by the motion of the blocks, which is coupled with the frictional heat generated by their movement (Hirono et al., 2008). This weak zone also facilitates the migration of fluids and the transfer of mantle heat due to the fractures. Therefore, the weak zone formed by the combined influence of tectonics and thermal structure contributes a favorable area for the formation of geothermal resources.

The presence of the Cenozoic cover acts as a protective barrier, minimizing heat loss and promoting the formation of geothermal resources in the Weihe Basin. From the focal depth profile of earthquakes (Figure 3B), it can be observed that all earthquakes occur below the cover layer, suggesting that the Cenozoic cover layer is relatively stable and not significantly affected by regional tectonics. Furthermore, the Cenozoic cover is composed of sandstone, conglomerate, and mudstone, which have low thermal conductivity (1.5–2.5 W/(m·K)); the pre-Cenozoic bedrock consists of limestone and dolomite, which have high thermal conductivity (3.5–4.5 W/(m·K)) (Ren et al., 2020). The low thermal conductivity of the Cenozoic cover retains heat and leads to its accumulation beneath the cover. Consequently, a promising reservoir of geothermal resources is formed beneath the Weihe Basin.

6 Conclusion

The outcomes of the present study unmistakably establish the correlation between earthquake occurrences and tectonic processes, deciphering the genesis of geothermal reservoirs within the Weihe Basin that are intricately associated with tectonic dynamics, elucidating the shared influence of regional tectonic activity in governing both the occurrence of earthquakes and the formation of geothermal reservoirs. The specific conclusions are as follows.

(i) A multitude of seismic events have been documented within the Weihe Basin. Their presence correlates with fault activity, and the formation and behavior of these faults are regulated by the movement of the regional blocks due to displacement, which in turn is attributed to the deformation of the Tibetan Plateau.

(ii) The geothermal resources in the Weihe Basin are partially derived from mantle heat conduction, while the other part is controlled by regional geological structures. Firstly, the subsurface movement of the deep asthenosphere can induce attenuation within the overlying lithosphere, giving rise to a region of thermal erosion. Concurrently, tectonic stresses contribute to the generation of an extensive network of faults and thermal erosion regions, thereby collaboratively establishing a zone of reduced mechanical strength. The weak zone facilitates fluid convection and forms favorable geothermal resources under the protection of the overlying Cenozoic cap rocks.

(iii) The occurrence of earthquakes and the formation of geothermal resources are jointly controlled by regional tectonics, exhibiting homologous characteristics and simultaneous manifestations. This finding provides new perspectives for future research endeavors in the realms of both geothermal exploration and earthquake investigations.

Data availability statement

The original contributions presented in the study are included in the article/Supplementary Material, further inquiries can be directed to the corresponding authors.

Author contributions

BZ: Data curation, Formal Analysis, Investigation, Methodology, Resources, Validation, Writing–original draft. YZ: Conceptualization, Project administration, Supervision, Writing–review and editing. JK: Conceptualization, Funding acquisition, Software, Supervision, Visualization, Writing–review and editing.

Funding

The author(s) declare financial support was received for the research, authorship, and/or publication of this article. This research is funded by the China Scholarship Council (No. 202106410023).

Acknowledgments

We are grateful to four reviewers for constructive reviews that greatly improved the manuscript; Fabio Luca Bonali for efficient editorial handling. Acknowledgements for the data support from "China Earthquake Networks Center, National Earthquake Data Center (http://data.earthquake.cn)", the United States Geological Survey (USGS), the GEOROC database (https://georoc.eu/georoc/new-start.asp), and International Heat Commission database (http://www.ihfc-iugg.org/products/global-heat-flow-database). Some figures are drawn by the Generic Mapping Tools version 6.3.0 (Wessel et al., 2019).

Conflict of interest

The authors declare that the research was conducted in the absence of any commercial or financial relationships that could be construed as a potential conflict of interest.

Publisher's note

Supplementary material

The Supplementary Material for this article can be found online at: https://www.frontiersin.org/articles/10.3389/feart.2024.1287450/full#supplementary-material

References

Ai, S., Zheng, Y., Riaz, M. S., Song, M., Zeng, S., and Xie, Z. (2019). Seismic evidence on different rifting mechanisms in southern and northern segments of the fenhe-weihe rift zone. *J. Geophys. Res. Solid Earth* 124 (1), 609–630. doi:10.1029/2018JB016476

Ai, Y., Zhang, J., Dong, M., Wang, B., and Fang, G. (2021). Heat generation effects from shear friction along Xianshui river strike-slip fault in western Sichuan, China. *Geothermics* 89, 101936. doi:10.1016/j.geothermics.2020.101936

An, M., and Shi, Y. (2006). Lithospheric thickness of the Chinese continent. *Phys. Earth Planet. Interiors* 159 (3), 257–266. doi:10.1016/j.pepi.2006.08.002

Bao, X., Xu, M., Wang, L., Mi, N., Yu, D., and Li, H. (2011). Lithospheric structure of the Ordos Block and its boundary areas inferred from Rayleigh wave dispersion. *Tectonophysics* 499 (1), 132–141. doi:10.1016/j.tecto.2011.01.002

Bea, F. (2012). The sources of energy for crustal melting and the geochemistry of heat-producing elements. *Lithos* 153, 278–291. doi:10.1016/j.lithos.2012.01.017

Chen, B., Liu, Y., Fang, L., Xu, S., Stuart, F. M., and Liu, C. (2023). A review of noble gas geochemistry in natural gas from sedimentary basins in China. *J. Asian Earth Sci.* 246, 105578. doi:10.1016/j.jseaes.2023.105578

Chen, Z., and Chen, Z. (2021). Identifying references to volcanic eruptions in Chinese historical records. *Geol. Soc. Lond. Spec. Publ.* 510 (1), 271–289. doi:10.1144/SP510-2020-86

Cheng, Y., He, C., Rao, G., Yan, B., Lin, A., Hu, J., et al. (2018). Geomorphological and structural characterization of the southern Weihe Graben, central China: implications for fault segmentation. *Tectonophysics* 722, 11–24. doi:10.1016/j.tecto.2017.10.024

Clark, M. K., and Royden, L. H. (2000). Topographic ooze: building the eastern margin of Tibet by lower crustal flow. *Geology* 28 (8), 703–706. doi:10.1130/0091-7613(2000)28<703:TOBTEM>2.0.CO;2

Deng, Y., and Levandowski, W. (2018). Lithospheric alteration, intraplate crustal deformation, and topography in eastern China. *Tectonics* 37 (11), 4120–4134. doi:10.1029/2018TC005079

Erfurt, P. (2021). "Hot springs throughout history," in *The geoheritage of hot springs. Geoheritage, geoparks and geotourism*. Editor P. Erfurt (Cham: Springer International Publishing), 119–182.

Fagereng, Å., and Biggs, J. (2019). New perspectives on 'geological strain rates' calculated from both naturally deformed and actively deforming rocks. *J. Struct. Geol.* 125, 100–110. doi:10.1016/j.jsg.2018.10.004

Feng, M., An, M., and Dong, S. (2017). Tectonic history of the Ordos block and qinling orogen inferred from crustal thickness. *Geophys. J. Int.* 210 (1), 303–320. doi:10.1093/gji/ggx163

Furlong, K. P., and Chapman, D. S. (2013). Heat flow, heat generation, and the thermal state of the lithosphere. *Annu. Rev. Earth Planet. Sci.* 41 (1), 385–410. doi:10.1146/annurev.earth.031208.100051

Gillis, K. M. (2008). The roof of an axial magma chamber: a hornfelsic heat exchanger. *Geology* 36 (4), 299–302. doi:10.1130/G24590A.1

Guo, X., Jiang, C., Han, L., Yin, H., and Zhao, Z. (2022a). *Focal mechanism data set in Chinese mainland and its adjacent area (2009-2021)*. Beijing: China Earthquake Administration. doi:10.12080/nedc.11.ds.2022.0004

Guo, Z., and Chen, Y. J. (2016). Crustal structure of the eastern Qinling orogenic belt and implication for reactivation since the Cretaceous. *Tectonophysics* 683, 1–11. doi:10.1016/j.tecto.2016.06.007

Guo, Z., Li, S., Yu, Y., Chen, Y. J., Yang, Y., Xu, B., et al. (2022b). Eastward asthenospheric flow from NE Tibet inferred by joint inversion of teleseismic body and surface waves: insight into widespread continental deformation in eastern China. *J. Geophys. Res. Solid Earth* 127 (8), e2022JB024410. doi:10.1029/2022JB024410

Hao, M., Wang, Q., Cui, D., Liu, L., and Zhou, L. (2016). Present-day crustal vertical motion around the Ordos block constrained by precise leveling and GPS data. *Surv. Geophys.* 37 (5), 923–936. doi:10.1007/s10712-016-9375-1

Harðardóttir, S., Halldórsson, S. A., and Hilton, D. R. (2018). Spatial distribution of helium isotopes in Icelandic geothermal fluids and volcanic materials with implications for location, upwelling and evolution of the Icelandic mantle plume. *Chem. Geol.* 480, 12–27. doi:10.1016/j.chemgeo.2017.05.012

Hasterok, D., and Chapman, D. S. (2011). Heat production and geotherms for the continental lithosphere. *Earth Planet. Sci. Lett.* 307 (1), 59–70. doi:10.1016/j.epsl.2011.04.034

Hasterok, D., and Webb, J. (2017). On the radiogenic heat production of igneous rocks. *Geosci. Front.* 8 (5), 919–940. doi:10.1016/j.gsf.2017.03.006

Hirn, A., Jiang, M., Sapin, M., Diaz, J., Nercessian, A., Lu, Q. T., et al. (1995). Seismic anisotropy as an indicator of mantle flow beneath the Himalayas and Tibet. *Nature* 375 (6532), 571–574. doi:10.1038/375571a0

Hirono, T., Fujimoto, K., Yokoyama, T., Hamada, Y., Tanikawa, W., Tadai, O., et al. (2008). Clay mineral reactions caused by frictional heating during an earthquake: an example from the Taiwan Chelungpu fault. *Geophys. Res. Lett.* 35 (16). doi:10.1029/2008GL034476

Huang, H.-H., Lin, F.-C., Schmandt, B., Farrell, J., Smith, R. B., and Tsai, V. C. (2015a). The Yellowstone magmatic system from the mantle plume to the upper crust. *Science* 348 (6236), 773–776. doi:10.1126/science.aaa5648

Huang, W., Lv, Y., Pierce, I. K. D., Su, S., and Peng, J. (2022). Cosmogenic age constraints on rock avalanches in the Qinling Range associated with paleoearthquake activity, central China. *Geomorphology* 413, 108347. doi:10.1016/j.geomorph.2022.108347

Huang, Z., and Chevrot, S. (2021). Mantle dynamics in the SE Tibetan Plateau revealed by teleseismic shear-wave splitting analysis. *Phys. Earth Planet. Interiors* 313, 106687. doi:10.1016/j.pepi.2021.106687

Huang, Z., Wang, P., Xu, M., Wang, L., Ding, Z., Wu, Y., et al. (2015b). Mantle structure and dynamics beneath SE Tibet revealed by new seismic images. *Earth Planet. Sci. Lett.* 411, 100–111. doi:10.1016/j.epsl.2014.11.040

Huang, Z., Xu, M., Wang, L., Mi, N., Yu, D., and Li, H. (2008). Shear wave splitting in the southern margin of the Ordos Block, north China. *Geophys. Res. Lett.* 35 (19). doi:10.1029/2008GL035188

Institute of Geophysics (1986). *Atlas of the historical earthquakes in China*. Beijing: SinoMaps Press.

Jello, J., and Baser, T. (2023). Utilization of existing hydrocarbon wells for geothermal system development: a review. *Appl. Energy* 348, 121456. doi:10.1016/j.apenergy.2023.121456

Jiang, G., Hu, S., Shi, Y., Zhang, C., Wang, Z., and Hu, D. (2019). Terrestrial heat flow of continental China: updated dataset and tectonic implications. *Tectonophysics* 753, 36–48. doi:10.1016/j.tecto.2019.01.006

Kato, A., and Ben-Zion, Y. (2021). The generation of large earthquakes. *Nat. Rev. Earth Environ.* 2 (1), 26–39. doi:10.1038/s43017-020-00108-w

Ke, T., Huang, S., Xu, W., and Li, X. (2021). Study on heat extraction performance of multiple-doublet system in Hot Sedimentary Aquifers: case study from the Xianyang geothermal field, Northwest China. *Geothermics* 94, 102131. doi:10.1016/j.geothermics.2021.102131

Kreemer, C., Blewitt, G., and Klein, E. C. (2014). A geodetic plate motion and global strain rate model. *Geochem. Geophys. Geosystems* 15 (10), 3849–3889. doi:10.1002/2014GC005407

Kuang, J., Wang, S., Qi, S., Xiao, Z., Zhang, M., and Wang, Y. (2020). Cenozoic tectonic evolution of South China: a brief review, and new insights from the Huangshadong-Shiba area, south-east China. *Geol. J.* 55 (12), 7716–7737. doi:10.1002/gj.3870

Li, M., Li, J., and Wei, Y. (2022). Lithospheric structure beneath the Qinling Orogenic Belt and its surrounding regions: implications for regional lithosphere deformation. *Terra nova.* 34 (1), 91–101. doi:10.1111/ter.12566

Li, Y., and Bürgmann, R. (2021). Partial coupling and earthquake potential along the Xianshuihe Fault, China. *J. Geophys. Res. Solid Earth* 126 (7), e2020JB021406. doi:10.1029/2020JB021406

Li, Y., Wu, Q., Pan, J., Zhang, F., and Yu, D. (2013). An upper-mantle S-wave velocity model for East Asia from Rayleigh wave tomography. *Earth Planet. Sci. Lett.* 377-378, 367–377. doi:10.1016/j.epsl.2013.06.033

Liang, H., Gao, R., and Xue, S. (2022). Lithospheric electrical structure and its implications for the evolution of the middle Qinling Orogenic Belt, Central China: constraints from 3-D magnetotelluric imaging. *Tectonophysics* 832, 229359. doi:10.1016/j.tecto.2022.229359

Lin, A., Rao, G., and Yan, B. (2015). Flexural fold structures and active faults in the northern–western Weihe Graben, central China. *J. Asian Earth Sci.* 114, 226–241. doi:10.1016/j.jseaes.2015.04.012

Liu, J., Zhang, P., Lease, R. O., Zheng, D., Wan, J., Wang, W., et al. (2013). Eocene onset and late Miocene acceleration of Cenozoic intracontinental extension in the North Qinling range–Weihe graben: insights from apatite fission track thermochronology. *Tectonophysics* 584, 281–296. doi:10.1016/j.tecto.2012.01.025

Liu, Q., Zhang, L., Zhang, C., and He, L. (2016). Lithospheric thermal structure of the North China Craton and its geodynamic implications. *J. Geodyn.* 102, 139–150. doi:10.1016/j.jog.2016.09.005

Lucazeau, F. (2019). Analysis and mapping of an updated terrestrial heat flow data set. *Geochem. Geophys. Geosystems* 20 (8), 4001–4024. doi:10.1029/2019GC008389

Lund, J. W., and Boyd, T. L. (2016). Direct utilization of geothermal energy 2015 worldwide review. *Geothermics* 60, 66–93. doi:10.1016/j.geothermics.2015.11.004

Lund, J. W., Freeston, D. H., and Boyd, T. L. (2011). Direct utilization of geothermal energy 2010 worldwide review. *Geothermics* 40 (3), 159–180. doi:10.1016/j.geothermics.2011.07.004

Lund, J. W., and Toth, A. N. (2021). Direct utilization of geothermal energy 2020 worldwide review. *Geothermics* 90, 101915. doi:10.1016/j.geothermics.2020.101915

Luo, L., Pang, Z., Liu, J., Hu, S., Rao, S., Li, Y., et al. (2017). Determining the recharge sources and circulation depth of thermal waters in Xianyang geothermal field in Guanzhong Basin: the controlling role of Weibei Fault. *Geothermics* 69, 55–64. doi:10.1016/j.geothermics.2017.04.006

Lv, Y., Peng, J., and Wang, G. (2014). Characteristics and genetic mechanism of the Cuihua Rock Avalanche triggered by a paleo-earthquake in northwest China. *Eng. Geol.* 182, 88–96. doi:10.1016/j.enggeo.2014.08.017

Ma, X., and Wu, D. (1987). Cenozoic extensional tectonics in China. *Tectonophysics* 133 (3), 243–255. doi:10.1016/0040-1951(87)90268-X

Molnar, P., and Tapponnier, P. (1975). Cenozoic Tectonics of Asia: effects of a Continental Collision: features of recent continental tectonics in Asia can be interpreted as results of the India-Eurasia collision. *Science* 189 (4201), 419–426. doi:10.1126/science.189.4201.419

Paternoster, M., Oggiano, G., Sinisi, R., Caracausi, A., and Mongelli, G. (2017). Geochemistry of two contrasting deep fluids in the Sardinia microplate (western Mediterranean): relationships with tectonics and heat sources. *J. Volcanol. Geotherm. Res.* 336, 108–117. doi:10.1016/j.jvolgeores.2017.02.011

Pollack, H. N., and Chapman, D. S. (1977). On the regional variation of heat flow, geotherms, and lithospheric thickness. *Tectonophysics* 38 (3), 279–296. doi:10.1016/0040-1951(77)90215-3

Qin, D., Turner, J. V., and Pang, Z. (2005). Hydrogeochemistry and groundwater circulation in the Xi'an geothermal field, China. *Geothermics* 34 (4), 471–494. doi:10.1016/j.geothermics.2005.06.004

Qu, F., Zhang, Q., Niu, Y., Lu, Z., Wang, S., Zhao, C., et al. (2022). Mapping the recent vertical crustal deformation of the Weihe Basin (China) using sentinel-1 and ALOS-2 ScanSAR imagery. *Remote Sens.* 14 (13), 3182. doi:10.3390/rs14133182

Qu, W., Lu, Z., Zhang, Q., Wang, Q., Hao, M., Zhu, W., et al. (2018). Crustal deformation and strain fields of the Weihe Basin and surrounding area of central China based on GPS observations and kinematic models. *J. Geodyn.* 120, 1–10. doi:10.1016/j.jog.2018.06.003

Rao, G., Lin, A., Yan, B., Jia, D., and Wu, X. (2014). Tectonic activity and structural features of active intracontinental normal faults in the Weihe Graben, central China. *Tectonophysics* 636, 270–285. doi:10.1016/j.tecto.2014.08.019

Ren, Z.-l., Liu, R.-c., Ren, W.-b., Qi, K., Yang, G.-l., Cui, J.-p., et al. (2020). Distribution of geothermal field and its controlling factors in the Weihe basin. *Acta Geol. Sin.* 94 (7), 1938–1949. (in Chinese with English abstract). doi:10.3724/SP.J.0001-571720200703

Rudnick, R. L., and Gao, S. (2003). "3.01 - composition of the continental crust," in *Treatise on geochemistry*. Editors H. D. Holland, and K. K. Turekian (Oxford: Pergamon), 1–64.

Shi, W., Dong, S., and Hu, J. (2020). Neotectonics around the Ordos Block, North China: a review and new insights. *Earth-Science Rev.* 200, 102969. doi:10.1016/j.earscirev.2019.102969

Si, X., Teng, J., Liu, Y., Ma, X., Qiao, Y., Dong, X., et al. (2016). Crust structure of the Qinling orogenic and the region on its north and south margins from teleseismic receiver function. *Chin. J. Geophys.* 59 (4), 1321–1334. (in Chinese with English abstract). doi:10.6038/cjg20160414

Sibson, R. H. (1986). Earthquakes and rock deformation in crustal fault zones. *Annu. Rev. Earth Planet. Sci.* 14 (1), 149–175. doi:10.1146/annurev.ea.14.050186.001053

Su, P., He, H., Liu, Y., Shi, F., Granger, D. E., Kirby, E., et al. (2023). Quantifying the structure and extension rate of the linfen basin, shanxi rift system since the latest miocene: implications for continental magma-poor rifting. *Tectonics* 42 (9), e2023TC007885. doi:10.1029/2023TC007885

Su, P., He, H., Tan, X., Liu, Y., Shi, F., and Kirby, E. (2021). Initiation and evolution of the shanxi rift system in north China: evidence from low-temperature thermochronology in a plate reconstruction framework. *Tectonics* 40 (3), e2020TC006298. doi:10.1029/2020TC006298

Tang, G.-J., Wyman, D. A., Dan, W., Wang, Q., Gadoev, M., and Oimahmadov, I. (2023). Magma migration and surface uplift in Pamir–western Tibet driven by deep lithospheric dynamics. *Geology* 51, 813–817. doi:10.1130/G51216.1

Tang, Y., Zhou, S., Chen, Y. J., Sandvol, E., Liang, X., Feng, Y., et al. (2015). Crustal structures across the western Weihe Graben, North China: implications for extrusion tectonics at the northeast margin of Tibetan Plateau. *J. Geophys. Res. Solid Earth* 120 (7), 5070–5081. doi:10.1002/2014JB011210

Tian, Q.-H., Zhang, W.-T., and Zhu, W. (2023). Characterizing crustal deformation of the Weihe Fault, Weihe Basin (Central China), using InSAR and GNSS observations. *Appl. Sci.* 13 (11), 6835. doi:10.3390/app13116835

Todrani, A., Speranza, F., D'Agostino, N., and Zhang, B. (2022). Post-50 ma evolution of India-Asia collision zone from paleomagnetic and GPS data: greater India indentation to eastward Tibet flow. *Geophys. Res. Lett.* 49 (1), e2021GL096623. doi:10.1029/2021GL096623

Tong, Y., Sun, Y., Wu, Z., Mao, C., Pei, J., Yang, Z., et al. (2018). Passive crustal clockwise rotational deformation of the Sichuan Basin since the Miocene and its relationship with the tectonic evolution of the fault systems on the eastern edge of the Tibetan Plateau. *GSA Bull.* 131 (1-2), 175–190. doi:10.1130/B31965.1

Wang, G., Liu, Y., Zhu, X., and Zhang, W. (2020). The status and development trend of geothermal resources in China. *Earth Sci. Front.* 27 (01), 1–9. (in Chinese with English abstract). doi:10.13745/j.esf.2020.1.1

Wang, L., Zhang, H., Zhang, D. D., Cheng, H., Zhang, S., Li, T., et al. (2023). New evidence of prehistoric human activity on the central Tibetan plateau during the early to middle Holocene. *Holocene* 33, 1196–1206. doi:10.1177/09596836231183060

Wang, M., and Shen, Z.-K. (2020). Present-day crustal deformation of continental China derived from GPS and its tectonic implications. *J. Geophys. Res. Solid Earth* 125 (2), e2019JB018774. doi:10.1029/2019JB018774

Wessel, P., Luis, J. F., Uieda, L., Scharroo, R., Wobbe, F., Smith, W. H. F., et al. (2019). The generic mapping Tools version 6. *Geochem. Geophys. Geosystems* 20 (11), 5556–5564. doi:10.1029/2019GC008515

Wu, S., Guo, Z., Chen, Y. J., and Morgan, J. P. (2022). Seismic constraints and geodynamic implications of differential lithosphere-asthenosphere flow revealed in East Asia. *Proc. Natl. Acad. Sci.* 119 (43), e2203155119. doi:10.1073/pnas.2203155119

Wu, Y.-B., and Zheng, Y.-F. (2013). Tectonic evolution of a composite collision orogen: an overview on the Qinling–Tongbai–Hong'an–Dabie–Sulu orogenic belt in central China. *Gondwana Res.* 23 (4), 1402–1428. doi:10.1016/j.gr.2012.09.007

Xu, J., Oppenheimer, C., Hammond, J. O. S., and Wei, H. (2021). Perspectives on the active volcanoes of China. *Geol. Soc. Lond. Spec. Publ.* 510 (1), 1–14. doi:10.1144/SP510-2021-87

Xu, P., Li, M., Qian, H., Zhang, Q., Liu, F., and Hou, K. (2019). Hydrochemistry and geothermometry of geothermal water in the central Guanzhong Basin, China: a case study in Xi'an. *Environ. Earth Sci.* 78 (3), 87. doi:10.1007/s12665-019-8099-1

Xu, W., Li, Y., Zhou, L., Ke, T., and Cheng, L. (2020). Lithospheric thermal regime under the qinling orogenic belt and the Weihe Basin: a transect across the yangtze and the North China cratons in central China. *Tectonophysics* 789, 228514. doi:10.1016/j.tecto.2020.228514

Xu, W., Tang, X., Cheng, L., Dong, Y., Zhang, Y., Ke, T., et al. (2022). Heat flow and thermal source of the xi'an depression, Weihe Basin, Central China. *Front. Earth Sci.* 9. doi:10.3389/feart.2021.819659

Yang, T., Monna, S., and Fang, L. (2022). Seismic imaging of the crust and uppermost mantle structure in the Qinling orogenic belt and its surroundings: geodynamic implications. *Tectonophysics* 843, 229619. doi:10.1016/j.tecto.2022.229619

Yi, M. (1993). The neotectonic movement and its basic characteristics in the Weihe graben basin. *Bull. Chin. Acad. Geol. Sci.* 27-28, 27–41. (in Chinese with English abstract).

Yin, A., and Harrison, T. M. (2000). Geologic evolution of the himalayan-Tibetan orogen. *Annu. Rev. Earth Planet. Sci.* 28 (1), 211–280. doi:10.1146/annurev.earth.28.1.211

Yin, A., and Taylor, M. H. (2011). Mechanics of V-shaped conjugate strike-slip faults and the corresponding continuum mode of continental deformation. *GSA Bull.* 123 (9-10), 1798–1821. doi:10.1130/B30159.1

Yu, Y., and Chen, Y. J. (2016). Seismic anisotropy beneath the southern Ordos block and the Qinling-Dabie orogen, China: eastward Tibetan asthenospheric flow around the southern Ordos. *Earth Planet. Sci. Lett.* 455, 1–6. doi:10.1016/j.epsl.2016.08.026

Yu, Y., Chen, Y. J., Feng, Y., An, M., Liang, X., Guo, Z., et al. (2021). Asthenospheric flow channel from northeastern Tibet imaged by seismic tomography between Ordos block and yangtze craton. *Geophys. Res. Lett.* 48 (17), e2021GL093561. doi:10.1029/2021GL093561

Zhang, W., Li, Y., Zhao, F., Han, W., Li, Y., Wang, Y., et al. (2019). Using noble gases to trace groundwater evolution and assess helium accumulation in Weihe Basin, central China. *Geochimica Cosmochimica Acta* 251, 229–246. doi:10.1016/j.gca.2019.02.024

Zhang, Y., Dong, S., Wang, H., Feng, M., Thybo, H., Li, J., et al. (2022). Coupled lithospheric deformation in the qinling orogen, Central China: insights from seismic reflection and surface-wave tomography. *Geophys. Res. Lett.* 49 (14), e2022GL097760. doi:10.1029/2022GL097760

Zhang, Y. G., Zheng, W. J., Wang, Y. J., Zhang, D. L., Tian, Y. T., Wang, M., et al. (2018). Contemporary deformation of the North China plain from global positioning system data. *Geophys. Res. Lett.* 45 (4), 1851–1859. doi:10.1002/2017GL076599

Zhao, K., Luo, Y., Yang, Y., and Yang, X. (2021). High-resolution lithospheric structures of the Qinling-Dabie orogenic belt: implications for deep subduction and delamination of continental lithosphere. *Tectonophysics* 806, 228799. doi:10.1016/j.tecto.2021.228799

Zhou, Z.-M., Ma, C.-Q., Qi, S.-H., Xi, Y.-F., and Liu, W. (2020). Late Mesozoic high-heat-producing (HHP) and high-temperature geothermal reservoir granitoids: the most significant geothermal mechanism in South China. *Lithos* 366-367, 105568. doi:10.1016/j.lithos.2020.105568

Zhu, J., Hu, K., Lu, X., Huang, X., Liu, K., and Wu, X. (2015). A review of geothermal energy resources, development, and applications in China: current status and prospects. *Energy* 93, 466–483. doi:10.1016/j.energy.2015.08.098